

Supporting Information

Probing Growth of Metal–Organic Frameworks with X-Ray Scattering and Vibrational Spectroscopy

Wenchao Lu,¹ Emily Zhang,^{1,2} Jin Qian,¹ Chaya Weeraratna,¹ Megan N. Jackson,² Chenhui Zhu,⁴ Jeffrey R. Long,^{2,3,5} and Musahid Ahmed.^{1,*}

¹ Chemical Sciences Division, Lawrence Berkeley National Laboratory, Berkeley, CA 94720, USA

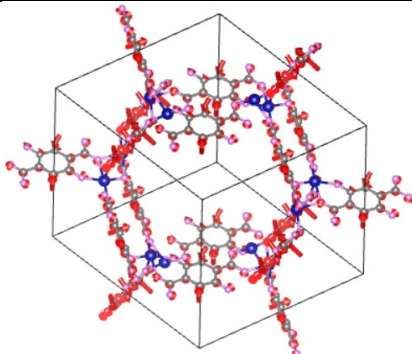
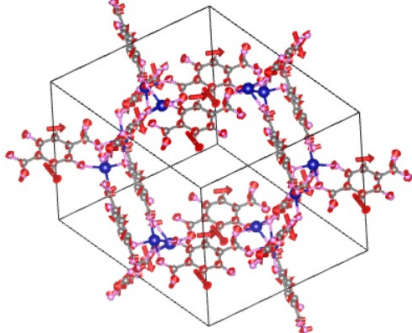
² Department of Chemistry, University of California, Berkeley, CA 94720, USA

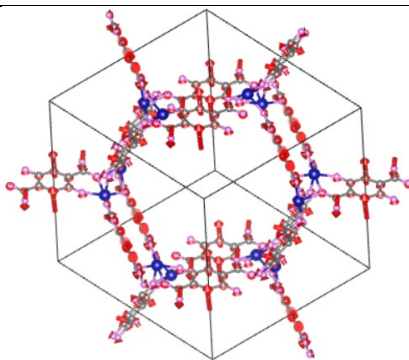
³ Material Sciences Division, Lawrence Berkeley National Laboratory, Berkeley, CA 94720, USA

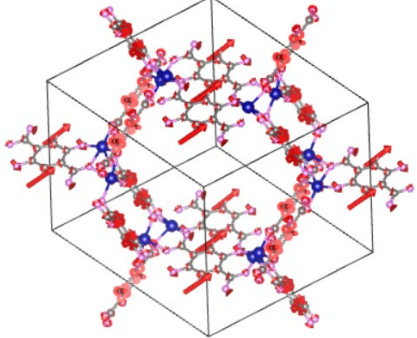
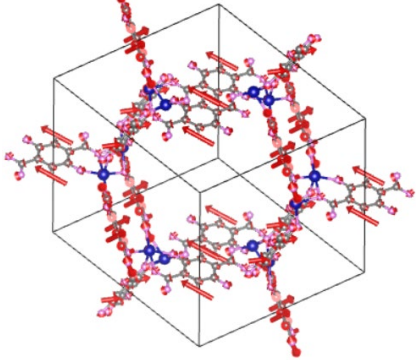
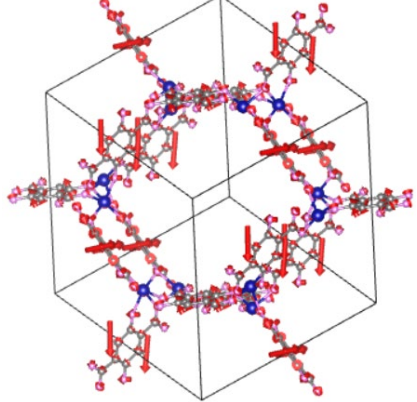
⁴ Advanced Light Source, Lawrence Berkeley National Laboratory, Berkeley, CA 94720, USA

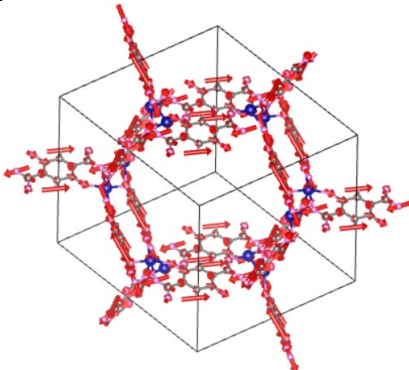
⁵Department of Chemical and Biomolecular Engineering, University of California, Berkeley, Berkeley, California 94720, United States

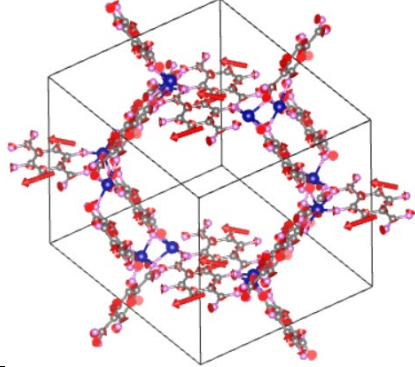
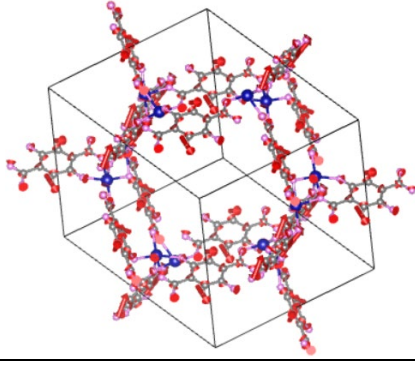
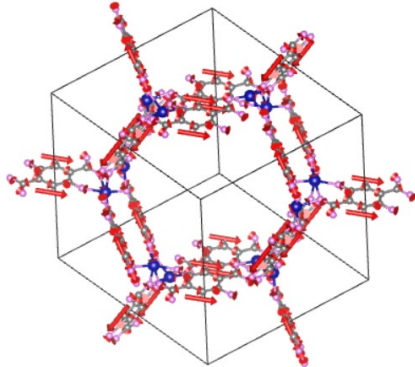
Table S1 Summary of IR vibrational modes from plane wave density functional theory. The modes with a relatively strong calculated IR intensity (> 0.35 a.u.) are marked in bold with the corresponding vibrational modes visualized by VESTA.¹

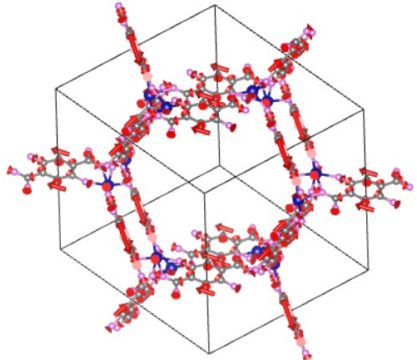
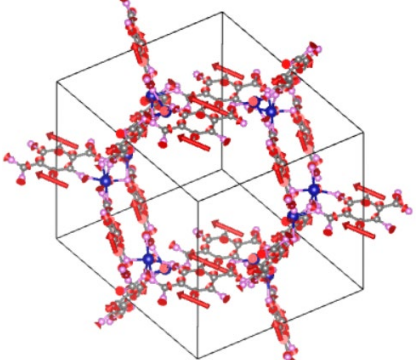
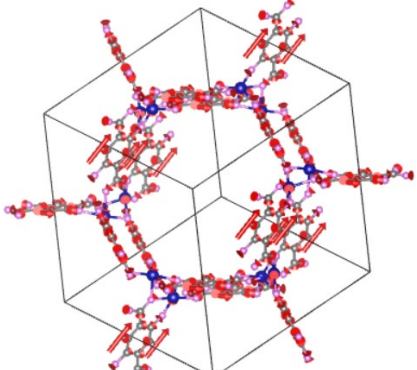
Mode	IR Frequency (cm^{-1})	IR Intensity (a.u.)	IR modes
159	44.89939562	0.00012884	
158	69.89106867	0.00098276	
157	91.90093685	0.00493982	
156	99.88233883	0.00570798	
155	100.7515809	0.01115111	
154	104.8097617	0.00187897	
153	107.7318572	0.02950086	
152	110.8425595	0.00242511	
151	119.96009	0.00907427	
150	125.4913263	0.02762092	
149	127.747235	0.01450917	
148	129.299053	0.0059868	
147	132.1039311	0.00263116	
146	137.8602098	0.0373124	
145	140.9170329	0.77113656	 <p>Collective phonon mode in the linker region of 2,5-dioxido-1,4-benzenedicarboxylate and Co cage</p>
144	144.3471107	0.05732724	
143	145.8934618	0.66139796	 <p>Collective phonon mode in the linker region of 2,5-dioxido-1,4-benzenedicarboxylate and Co cage</p>
142	149.0760778	0.03494518	

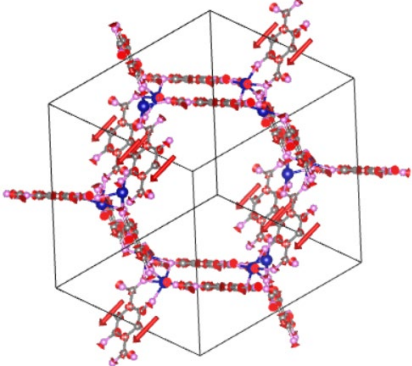
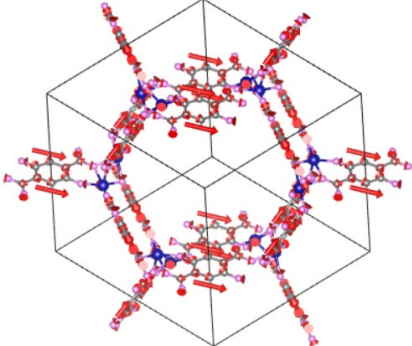
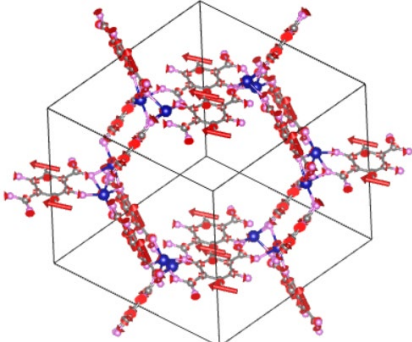
141	152.1470209	0.00351805	
140	160.6784979	0.02548824	
139	164.8299145	2.0185E-05	
138	166.6137528	0.00039777	
137	168.04494	0.01179172	
136	171.8648899	0.00106051	
135	173.0560467	0.00260825	
134	186.610406	0.16500442	
133	189.0694765	0.02013146	
132	190.72775	0.74014256	 <p>Collective phonon mode in the linker region of 2,5-dioxido-1,4-benzenedicarboxylate and Co cage</p>
131	196.5897263	0.00035129	
130	197.9043777	0.00362534	
129	201.4130482	0.00090381	
128	213.5747415	0.14371982	
127	214.2673285	0.15198421	
126	219.1595128	0.00409503	
125	228.0082435	5.5878E-05	
124	228.7329145	1.9708E-05	
123	231.1790553	0.00027637	
122	238.1140353	0.00376331	
121	239.2238757	0.0007933	
120	240.2491969	0.03903663	
119	250.2264717	0.00029656	
118	253.2930853	4.3278E-05	
117	260.7613821	0.09285504	
116	262.7475289	0.07043842	
115	269.6880722	0.00102128	

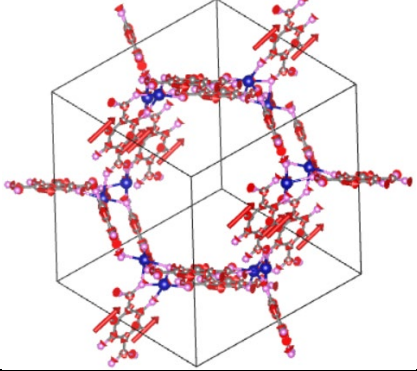
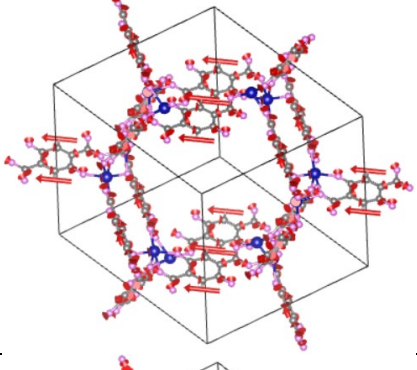
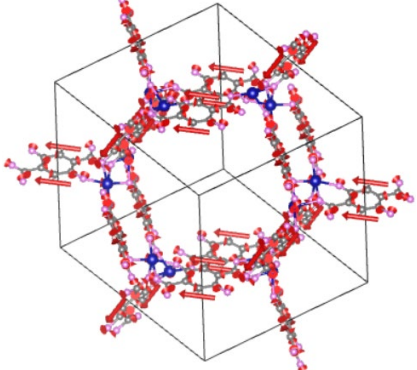
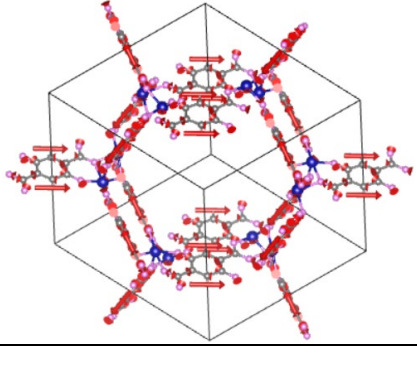
114	278.9878413	0.45506196	 <p>Hexagonal pore-breathing mode along direction roughly parallel to c</p>
113	282.0713103	0.54689371	 <p>Hexagonal pore-breathing mode along direction roughly parallel to a</p>
112	283.0122301	0.58574538	 <p>Hexagonal pore-breathing mode along direction roughly parallel to b</p>
111	291.9640663	0.27690577	
110	327.4274555	0.03304656	
109	330.3083384	0.04897022	
108	345.1640134	2.6753E-05	
107	349.5066209	8.1682E-05	
106	350.898105	2.0596E-05	
105	390.1670278	1.4173E-05	
104	400.3509843	1.2651E-05	
103	401.8061877	1.9481E-05	

102	424.3176284	2.3223E-06	
101	428.3215856	4.7593E-06	
100	428.8938086	7.6604E-07	
99	441.2558	0.03654387	
98	442.4308938	0.02554369	
97	444.6822588	0.16057142	
96	463.2107967	0.03036975	
95	464.0733175	0.02706189	
94	465.3791943	0.01061877	
93	480.1172231	2.4088E-05	
92	480.5267092	4.1668E-05	
91	482.0395739	1.7966E-06	
90	512.3093945	0.46347477	
89	524.8130019	0.04158308	
88	526.2450205	0.04096185	
87	539.5446473	4.4614E-06	
86	544.9314226	5.5871E-06	
85	546.4718604	5.6393E-06	
84	560.4924639	0.03992793	
83	561.3216877	0.04395291	
82	562.784136	0.04732448	
81	615.0307296	0.01959397	
80	615.378708	0.03007678	
79	615.9224692	0.06909331	
78	641.9214497	3.1056E-05	
77	643.4500029	1.9164E-05	
76	644.159201	4.1789E-06	
75	689.073504	8.9084E-06	
74	689.4171028	1.6965E-06	
73	690.3225216	1.103E-06	
72	700.7047646	1.1481E-05	
71	701.17183	1.5245E-06	
70	702.2468544	1.2662E-05	
69	771.3168674	0.00018941	

68	771.9617255	0.00014301	
67	772.3695414	1.057E-05	
66	776.730906	0.04983059	
65	777.4254908	0.12215373	
64	777.7473754	0.13014841	
63	784.8736862	0.73519214	
62	785.777905	0.26447609	
61	786.1087851	0.63153506	
60	787.4017423	0.00854835	
59	787.8258914	0.02354002	
58	788.2615156	0.03660981	
57	854.2168142	0.25396803	
56	855.3892675	0.26197679	
55	859.4859207	0.39104733	
54	917.7478858	0.00239153	
53	918.7753812	1.4507E-05	
52	919.1057471	5.0048E-05	
51	929.2373644	0.04158793	

50	929.730912	0.0801139	
49	929.9957541	0.04814069	
48	1026.025598	8.9711E-06	
47	1031.937762	2.2011E-06	
46	1034.366474	3.1059E-06	
45	1100.798954	0.0120733	
44	1102.435467	0.0087699	
43	1103.368867	0.03854373	
42	1152.09021	0.94245142	
41	1155.829504	0.85835155	
40	1156.89789	0.85621298	
39	1206.968893	6.4677E-06	
38	1211.663155	1.9805E-06	
37	1213.951337	1.44E-05	
36	1223.702831	9.9918E-05	
35	1224.731752	3.4982E-05	
34	1225.248228	3.9363E-05	

33	1235.002941	0.19508844	
32	1237.711398	0.19198975	
31	1240.006968	0.07085211	
30	1306.577472	0.59928488	 A ball-and-stick model of a complex organic molecule, likely a porphyrin derivative, shown within a 3D wireframe unit cell. The molecule features a central macrocyclic ring with four nitrogen atoms (blue) coordinated to a central metal atom (grey). Various side chains are attached to the ring, including methyl (red/white) and ethyl (red/white) groups, and a long aliphatic chain. The unit cell is a rectangular prism.
29	1309.872341	0.58636532	 A ball-and-stick model of a complex organic molecule, similar to compound 30, shown within a 3D wireframe unit cell. The molecule features a central macrocyclic ring with four nitrogen atoms (blue) coordinated to a central metal atom (grey). Various side chains are attached to the ring, including methyl (red/white) and ethyl (red/white) groups, and a long aliphatic chain. The unit cell is a rectangular prism.
28	1312.404664	0.13789428	
27	1328.980588	2.1323E-05	
26	1333.211155	6.4583E-06	
25	1334.506104	7.0289E-06	
24	1346.296067	3.17709356	 A ball-and-stick model of a complex organic molecule, similar to compounds 30 and 29, shown within a 3D wireframe unit cell. The molecule features a central macrocyclic ring with four nitrogen atoms (blue) coordinated to a central metal atom (grey). Various side chains are attached to the ring, including methyl (red/white) and ethyl (red/white) groups, and a long aliphatic chain. The unit cell is a rectangular prism.

23	1348.400258	3.17263834	
22	1365.325097	0.16075598	
21	1407.605362	0.0004109	
20	1409.080672	0.00059312	
19	1411.304765	0.00073915	
18	1414.86685	0.92654523	
17	1416.719098	0.96448533	
16	1420.867193	0.38798031	

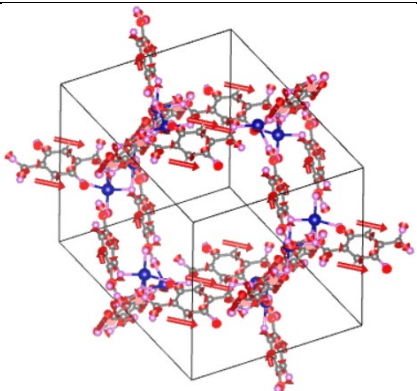
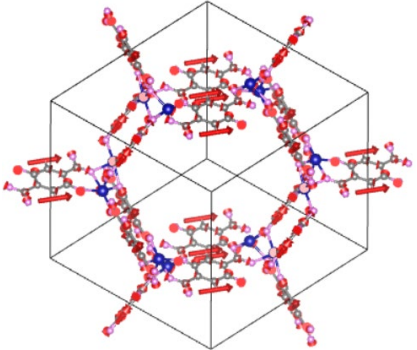
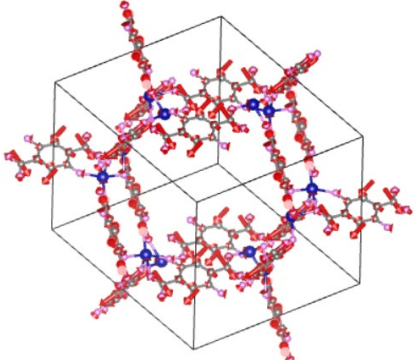
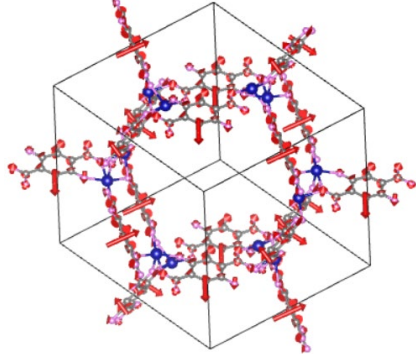
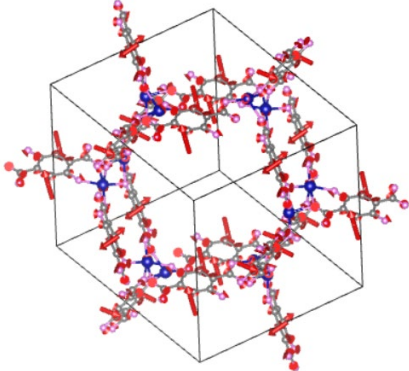
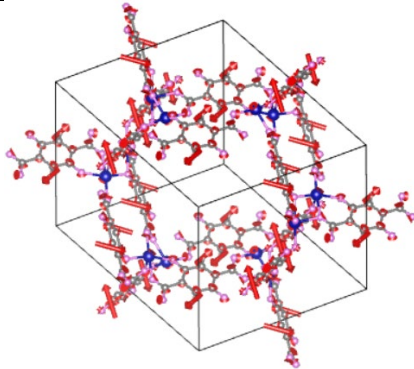
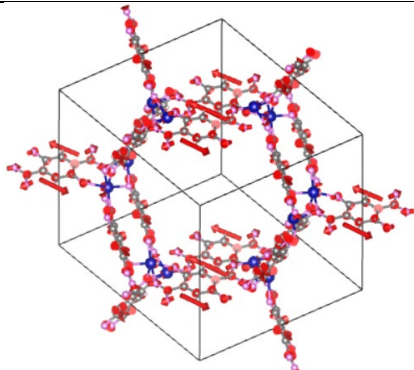
15	1432.087161	0.43863327	
14	1433.636712	0.45077141	
13	1439.847004	3.33615033	
12	1460.57452	8.6558E-05	
11	1461.808465	1.103E-05	
10	1462.657805	1.7882E-05	
9	1549.54054	4.0843E-06	
8	1554.119932	5.2392E-07	
7	1554.92839	7.0647E-08	
6	3053.415928	0.00356806	
5	3054.106817	0.01619123	
4	3054.826529	0.00309442	
3	3055.353283	0.01715966	
2	3057.18507	0.00565089	
1	3057.970841	0.01380634	

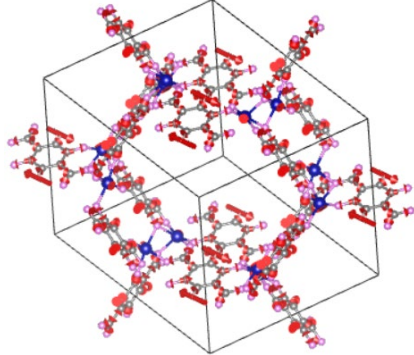
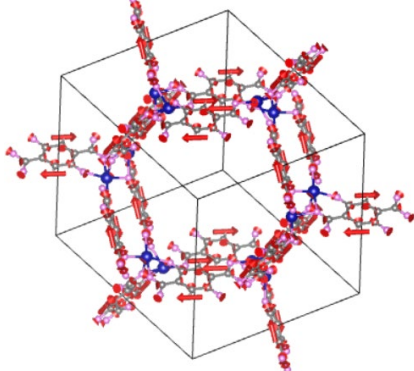
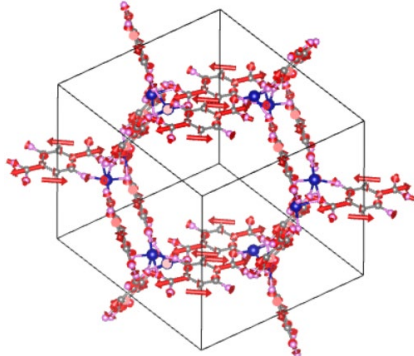
Table S2 Summary of Raman modes from plane wave density functional theory. The modes with a relatively strong calculated Raman activity ($>10^6 \text{ \AA}^4/\text{amu}$)² are shown in bold with the corresponding vibrational modes visualized by VESTA.¹

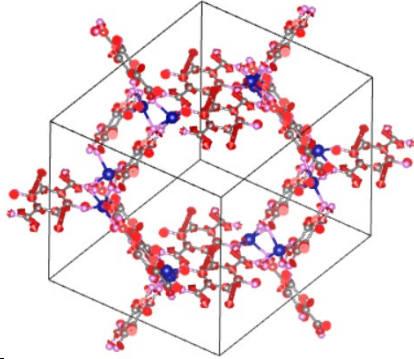
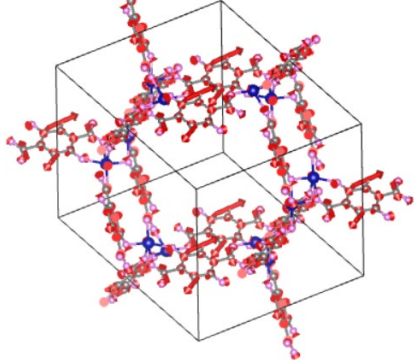
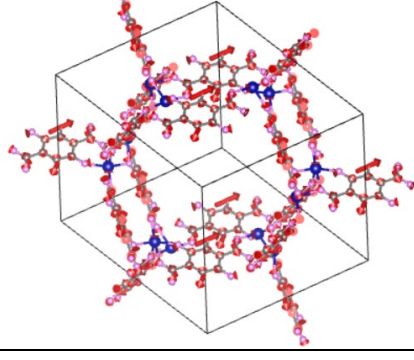
Mode	Raman Frequency (cm^{-1})	Raman Activity ($(\text{\AA}^4/\text{amu})$)	Raman modes
159	50.95853	42.7831304	
158	73.17858	3887.204694	
157	98.58957	202511.4592	
156	102.24176	3247.907912	
155	103.24998	20462.881	
154	103.4844	15758.0594	
153	104.12354	11523.72665	
152	109.81798	86.7702279	
151	120.27707	803159.1367	
150	125.77558	164.739671	
149	126.62085	169.2136437	
148	135.03432	27616.01482	
147	135.21377	29023.21298	
146	136.19814	2353.382596	
145	136.90995	48541.76398	
144	142.21758	683.0248445	
143	143.50259	118.2224174	
142	148.1633	48532.48694	
141	148.81738	51212.89333	
140	161.95643	166.0538464	
139	165.58783	3911.004619	
138	165.80406	1474.017168	
137	169.08246	57965.34168	
136	169.3876	78640.82615	
135	170.52264	1608492.005	
134	188.68781	211.2982253	
133	189.02899	342.8069268	
132	189.90438	155.7508547	
131	197.52759	36027.05748	
130	198.05931	35969.13184	

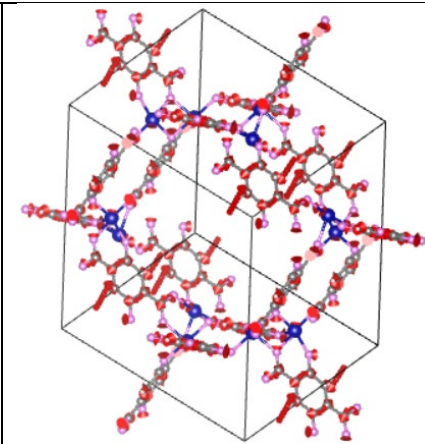
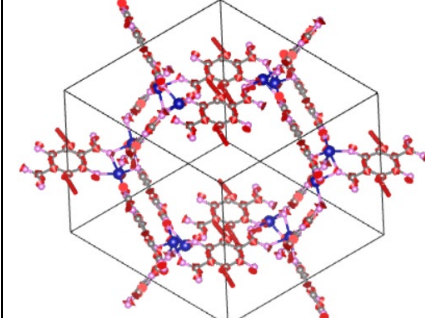
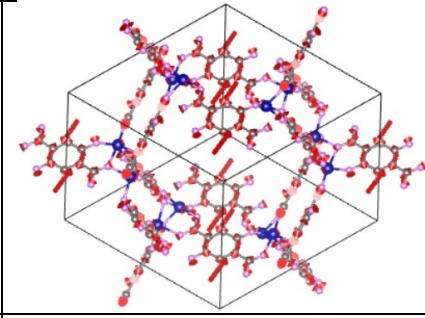
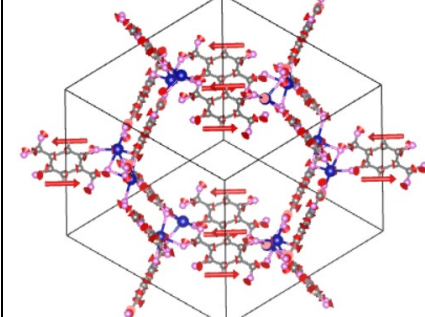
129	202.75072	744987.8808	
128	214.26762	235.0499693	
127	214.41285	1238.795329	
126	219.0457	155.0741647	
125	230.16836	176018.0944	
124	231.09404	151053.7682	
123	233.13055	9226783.319	
122	238.62626	35421.98101	
121	238.7555	42396.30289	
120	242.59832	2215.682524	
119	253.08179	69098.18137	
118	253.46529	75998.08353	
117	262.0922	226.0987004	
116	262.2039	265.7693703	
115	270.73772	273885.8532	
114	281.0877	145.2082119	
113	281.6534	56.5585057	
112	282.20258	138.6611465	
111	294.34856	48.4023262	
110	330.63864	171.8719926	
109	331.51394	92.6625941	
108	346.71451	43266.94373	
107	351.09553	48017.7061	
106	351.85849	44030.43389	
105	391.3746	9992.92782	
104	401.93752	45760.30137	
103	402.63196	42076.02375	

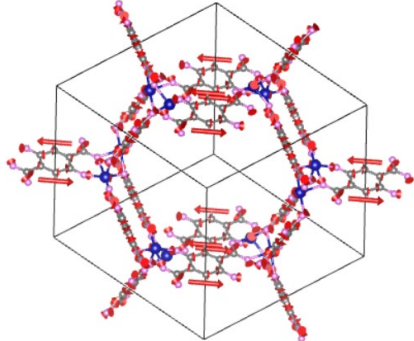
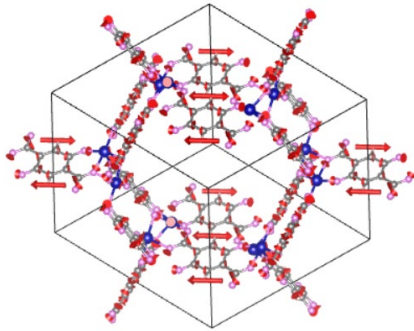
102	425.02904	2528321.673	
101	428.90642	111360.0438	
100	429.89606	100600.5836	
99	443.13279	286.0993106	
98	443.42612	230.3499826	
97	446.15729	475.8821067	
96	465.37264	1191.574368	
95	466.25512	650.437851	
94	466.92951	493.0047535	
93	480.88396	418355.4	
92	481.13723	186757.2088	
91	481.89795	8040001.843	
90	512.68457	160.7922822	
89	525.33486	198.478518	
88	526.16607	131.228375	
87	544.35796	364688.1038	
86	545.84206	105419.4683	
85	546.28189	95571.34593	
84	561.80799	132.3148946	
83	562.00872	199.8426764	
82	562.16254	70.5249201	
81	615.1113	369.6392695	
80	615.37354	253.8918785	
79	615.84745	55.9145654	
78	642.76403	7054.147573	
77	643.30051	26687.88784	

76	643.4371	25030.19134	
75	689.30105	8466.157443	
74	689.77596	16903.28135	
73	690.64667	177759.2437	
72	700.42075	34718.93275	
71	700.95926	37378.27357	
70	701.95807	99815.40539	
69	771.73576	21657.36065	
68	771.88862	25670.08836	
67	772.1635	26158.12347	
66	776.77393	225.8398847	
65	777.34586	283.1309266	
64	777.41232	195.6024403	
63	785.17597	6263.907045	
62	785.56341	95584.00084	
61	785.72316	915087.545	
60	787.05624	54787.54537	
59	787.42345	35120.22936	
58	788.38379	3896.036962	
57	853.77157	359.2667489	
56	854.53921	168.7127147	
55	858.44004	53.5609775	
54	916.86579	7055.741258	
53	918.10122	4037.701584	
52	920.02356	4593.765313	
51	927.55036	281.3558127	
50	928.31148	331.9314569	
49	930.33125	557.7970704	
48	1026.3432	259189.1511	
47	1031.17742	32614.79259	
46	1032.87649	14623.64345	
45	1100.67015	708.554544	
44	1101.09373	527.2214478	
43	1101.6371	431.039719	
42	1150.65368	293.4883208	
41	1153.08135	140.8100342	
40	1154.50869	298.3985869	

39	1207.63837	8302132.835	
38	1211.16864	4768434.303	
37	1212.37203	844427.0546	
36	1221.81625	154645.2011	
35	1222.38802	29443.59646	
34	1223.14816	84175.46879	
33	1235.02472	288.6190655	
32	1237.38016	116.8987354	
31	1238.33202	498.0149254	
30	1306.15933	156.5192937	
29	1309.01271	195.6929275	
28	1310.71262	303.3481649	
27	1327.42885	729937.7742	
26	1329.81471	739365.4503	
25	1333.25766	4192678.448	
24	1344.82829	204.0789085	
23	1346.83248	475.963979	
22	1361.5288	39.9315138	

21	1407.99711	1146712.492	
20	1408.99841	1159093.897	
19	1411.23321	3723156.955	
18	1413.53909	3594.596947	
17	1415.36005	2275.814781	
16	1418.77438	78.3495954	
15	1431.98043	214.7232618	
14	1433.28525	268.2464918	
13	1439.92207	91.3383666	

12	1460.98531	5787329.071	
11	1461.88864	5101940.907	
10	1462.58582	4757345.728	
9	1549.56485	1090728.326	

8	1553.53556	988088.2523	
7	1554.63132	1603107.296	
6	3042.01987	592.6514989	
5	3042.70778	305.977155	
4	3045.42092	1189.599409	
3	3047.86847	767.5525217	

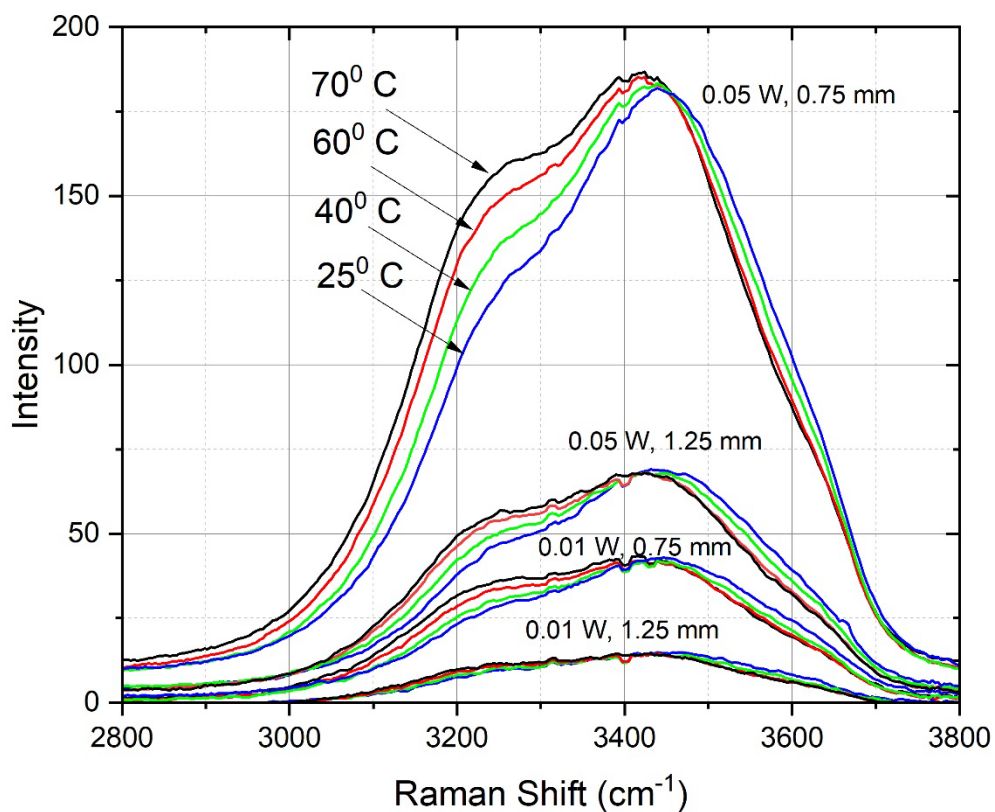


Figure S1 Raman spectroscopy of water in capillary under different laser focusing and power conditions marked in figure. Distance denoted is between capillary and focusing lens.

Smith et al.³ has performed Raman thermometry from liquid water droplets to determine the temperature, since the OH stretch frequencies are very sensitive to temperature between 3000-3800 cm^{-1} . The capillary was filled with water and the heater temperature adjusted to four temperatures. Upon comparison to the Smith et al. data, we build an effective temperature scale for our reactor based on the four measurements shown in Figure S1.

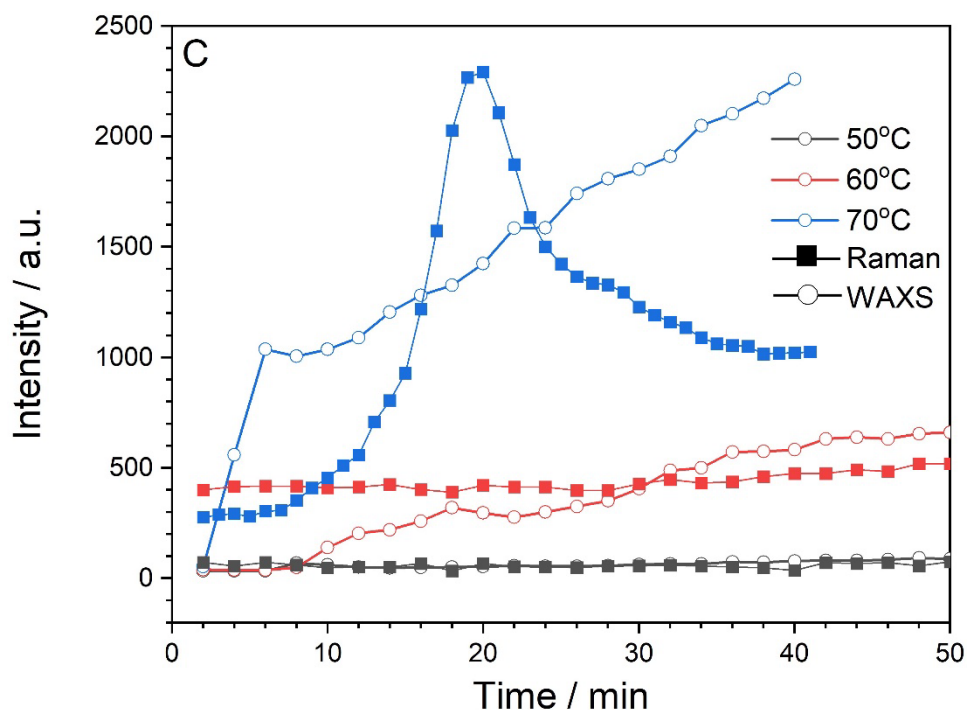


Figure S2. WAXS and Raman kinetic traces at heater temperature of 50, 60 and 70 °C. The WAXS kinetic traces are tracking the peak at 0.5 \AA^{-1} , and the Raman kinetic traces are tracking the peak at 1278 cm^{-1} .

WAXS and Raman kinetics: To trace the growth kinetics from the WAXS and Raman spectra, shown in Figure 3A and B, we plotted the time dependence of signal, 0.5 \AA^{-1} for WAXS, and the in-plane C-H bending mode intensity (1278 cm^{-1}) for Raman at three temperatures, 50, 60 and 70 °C. At a qualitative level, the signal shows a dependence on temperature, there is no discernable reaction at 50 °C, for the WAXS data at 60 °C there is a rise of signal at around the 8 min interval that gradually increases, while the signal at 70 °C is dramatic for WAXS with an onset around 2 minute and then plateaus at around the 6 min mark, and then continues to increase at a less rapid rate. The 70 °C signal from the Raman spectra is not so dramatic, with an onset around the 6 min mark, and then a rapid rise at the 10-minute mark, followed by depletion of signal around 20 minutes.

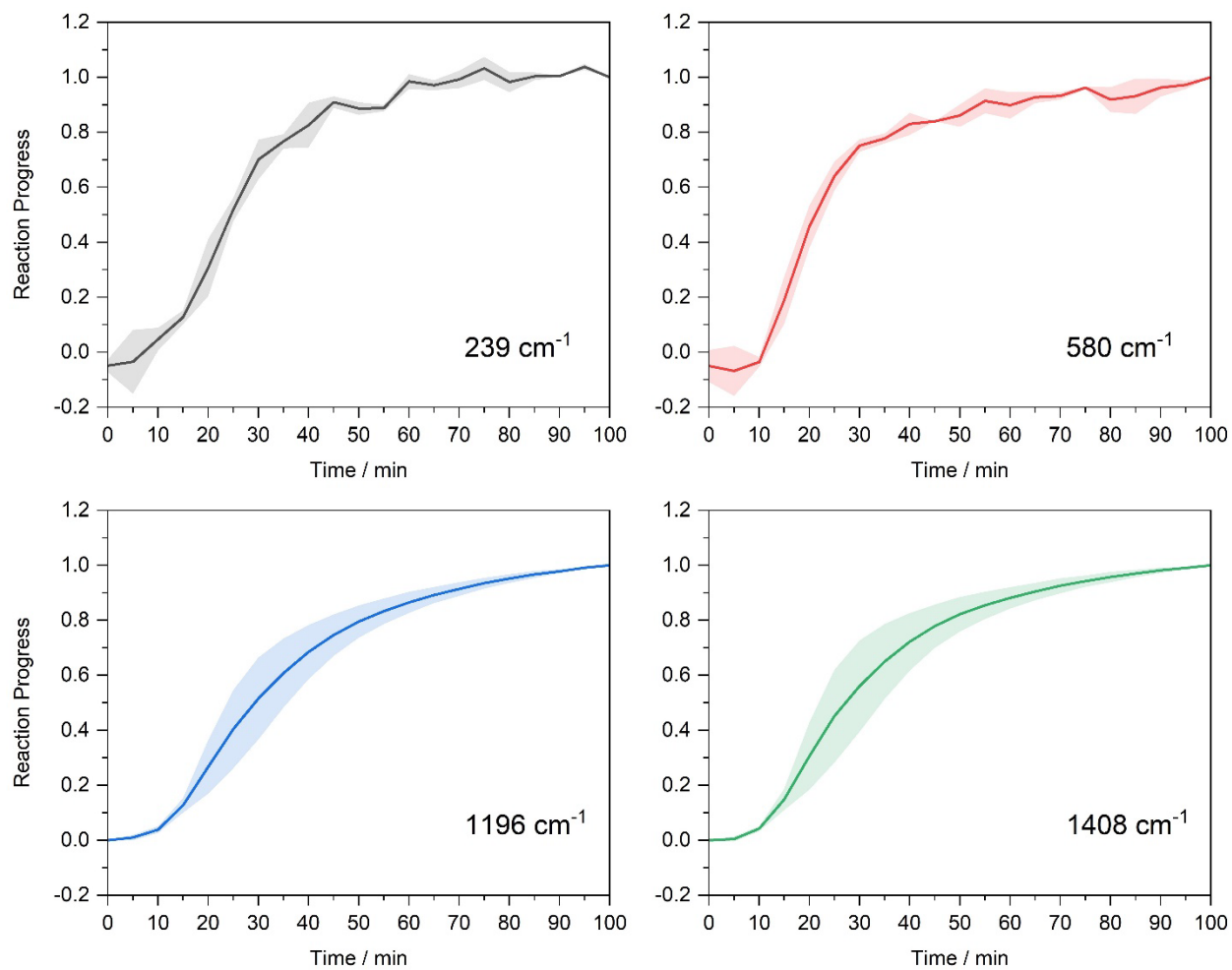


Figure S3 Errors of the MOF synthesis kinetics of 60°C measured by FIR and MIR at 239, 580, 1196 and 1480 cm⁻¹ from a set of three measurements.

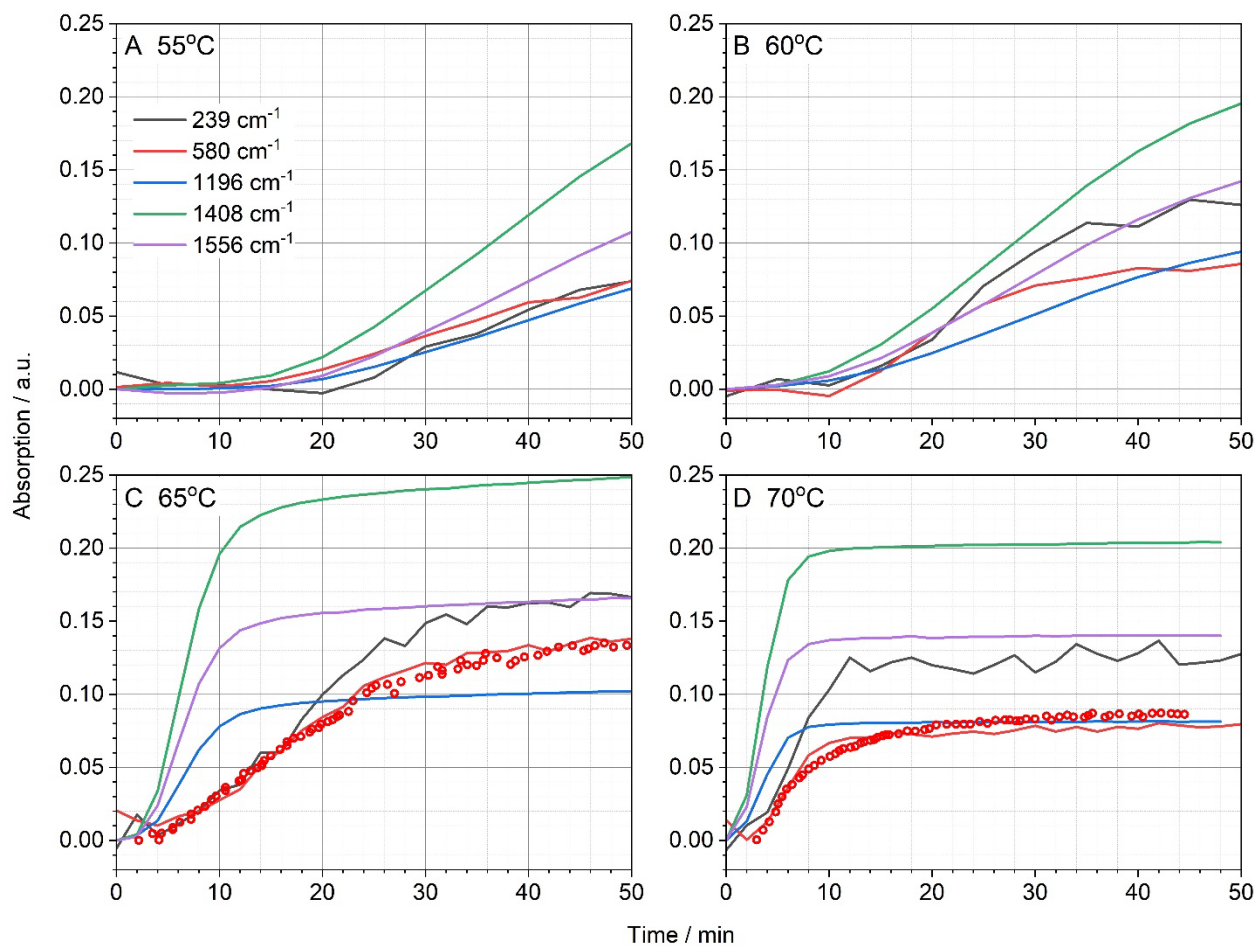


Figure S4 Absorption intensity of five FIR and MIR peaks as a function of time at temperatures of (A) 55 °C, (B) 60 °C, (C) 65 °C, (D) 70 °C. Black Line: 239 cm⁻¹, red line: 580 cm⁻¹, blue line 1196 cm⁻¹, Green line: 1408 cm⁻¹, magenta line: 1566 cm⁻¹. The red symbols in (C) and (D) are digitized data of X-Ray diffraction measurements of Co-MOF growth at 70 °C and 80 °C respectively from Osta et al.⁴

Table S3 Gualtieri model fitted kinetic parameters for the reaction traced by ATR-FTIR absorption intensity of 239, 580, 1196, 1408, and 1556 cm^{-1} .

239 cm^{-1}	55°C	60°C	65°C	70°C	75°C
<i>a</i>	35	23	13	5	3.8
<i>b</i>	7	5	5	1.5	0.8
<i>k_g</i>	0.02	0.05	0.06	0.17	0.42
<i>k_n</i>	0.028571	0.043478	0.076923	0.2	0.263158

580 cm^{-1}	55°C	60°C	65°C	70°C	75°C
<i>a</i>	25	17	11	5	2.8
<i>b</i>	7	5.5	5	1	0.6
<i>k_g</i>	0.02	0.05	0.06	0.17	0.42
<i>k_n</i>	0.04	0.058824	0.090909	0.2	0.357143

1196 cm^{-1}	55°C	60°C	65°C	70°C	75°C
<i>a</i>	36	26	5	3.6	4
<i>b</i>	11	10	1.6	0.8	2
<i>k_g</i>	0.018	0.036	0.14	0.4	0.35
<i>k_n</i>	0.027778	0.038462	0.2	0.277778	0.25

1408 cm^{-1}	55°C	60°C	65°C	70°C	75°C
<i>a</i>	34	25	5	3.6	4
<i>b</i>	12	11	1.3	0.8	2
<i>k_g</i>	0.02	0.039	0.15	0.4	0.45
<i>k_n</i>	0.029412	0.04	0.2	0.277778	0.25

1556 cm^{-1}	55°C	60°C	65°C	70°C	75°C
<i>a</i>	37	25	5	3	4
<i>b</i>	12	11	1.3	0.8	2
<i>k_g</i>	0.02	0.039	0.15	0.4	0.45
<i>k_n</i>	0.027027	0.04	0.2	0.333333	0.25

The Gualtieri model fitting resulted in different kinetic parameter sets for each wavenumber. In FIR region, the two wavenumbers, 239 (hexagonal pore-breathing mode) and 580 cm^{-1} (Co-O stretching) have similar kinetic parameters showing the nucleation kinetics starting from the cobalt core. The other three wavenumbers, 1196, 1408, and 1556 cm^{-1} in MIR region correspond to the growth kinetics of the skeleton and share similar kinetic parameters. Such facts indicate that the formation of Co-O bonds plays a central role in the nucleation process and determines the overall reaction rate, whereas the formation of ligand skeletons is more sensitive to the temperature change and becomes temperature-independent above 70°C.

References:

1. K. Momma and F. Izumi, *Journal of Applied Crystallography*, 2011, **44**, 1272-1276.
2. J. Neugebauer, M. Reiher, C. Kind and B. A. Hess, *Journal of Computational Chemistry*, 2002, **23**, 895-910.
3. J. D. Smith, C. D. Cappa, W. S. Drisdell, R. C. Cohen and R. J. Saykally, *J Am Chem Soc*, 2006, **128**, 12892-12898.
4. R. El Osta, M. Feyand, N. Stock, F. Millange and R. I. Walton, *Powder Diffraction*, 2013, **28**, S256-S275.